DSC MR Perfusion at 7T MRI: An Initial Single-Center Study for Validity and Practicability

Clare E. Buntrock, Ceren Dinçer, Onur Tuncer, Matthew White, Alexis Swensen, Mark Folkertsma and Can Özütemiz

AJNR Am J Neuroradiol published online 20 February 2025
http://www.ajnr.org/content/early/2025/02/20/ajnr.A8513

Published February 20, 2025 as 10.3174/ajnr.A8513

ORIGINAL RESEARCH
ULTRA-HIGH-FIELD MRI/IMAGING OF EPILEPSY/DEMYELINATING DISEASES/INFLAMMATION/INFECTION

DSC MR Perfusion at 7T MRI: An Initial Single-Center Study for Validity and Practicability

Clare E. Buntrock, Ceren Dinçer, Onur Tuncer, Matthew White, Alexis Swensen, Mark Folkertsma, and Can Özütemiz

ABSTRACT

BACKGROUND AND PURPOSE: DSC perfusion is an advanced imaging technique routinely used at 1.5T and 3T MRI. However, its utility is not well known in 7T MRI systems. We aim to evaluate if DSC perfusion is a valid and practicable tool at 7T MRI.

MATERIALS AND METHODS: A successful DSC perfusion was performed in 9 patients with an FDA-approved 7T MRI system (Siemens Terra with 1tx/32rx Nova head coil) in 2023. Half-dose contrast was administered by hand, followed by saline flush. Acquisition was initiated 45 seconds before contrast injection. Voxel size was 1.5 × 1.5 × 1.6 mm^3. Perfusion maps were generated by using either SyngoVia or DynaSuite software. Parameters including relative CBV (rCBV), relative CBF (rCBF), relative MTT (rMTT), and relative TTP (rTTP) were measured in 5 anatomic locations bilaterally (precentral gyrus, middle frontal gyrus, corona radiata, thalamus, occipital cortex) and enhancing lesions if present. Normalized ratios of rCBV (nrCBV), rCBF (nrCBF), rMTT (nrMTT), and rTTP (nrTTP) were calculated and compared on boxplots. Two neuroradiologists reviewed each scan visually by using a 5-point Likert scale regarding imaging quality and artifacts. Qualitative and quantitative assessments were made on DSC perfusion in cases with enhanced target lesions.

RESULTS: Uploading the source images to imaging software took approximately 30 minutes to a few hours. In a few circumstances, large data caused software crashes. Map generation took approximately 10–15 minutes. Susceptibility artifacts varied from mild to moderate in cerebellum, temporal lobes, brainstem, and basal ganglia and none to minimal in the frontal, occipital, and parietal gyri. Map quality was excellent to reasonably good for all cases. The nrCBV, nrCBF, nrMTT, and nrTTP resulted in similar measurements for each anatomic area. Six target lesions were assessed in 2 different patients with well to excellent visualization on fused maps. Three lesions were characterized as tumor progression (1 biopsy-confirmed, 2 unconfirmed), 1 lesion as indeterminant (regressed in follow-up), and 2 lesions as radiation necrosis (1 stable, 1 regressed on follow-up).

CONCLUSIONS: Despite limitations with postprocessing issues, it is possible to reliably measure nrCBV, nrCBF, nrMTT, and nrTTP values with DSC perfusion by using a clinical 7T MRI system, and qualitatively, excellent or reasonably good fusion maps can be generated with high resolution.

ABBREVIATIONS: ASFNR = American Society of Functional Neuroradiology; GBCA = gadolinium-based contrast agent; GRE = gradient echo; NAWM = normal-appearing white matter; nrCBF = normalized ratio of relative CBF; nrCBV = normalized ratio of relative CBV; nrMTT = normalized ratio of relative MTT; nrTTP = normalized ratio of relative TTP; rCBF = relative CBF; rCBV = relative CBV; rMTT = relative MTT; rTTP = relative TTP

DSC perfusion is an advanced MRI technique routinely implemented and established at clinical 1.5T and 3T MRI to study brain function and intracranial lesions.[1-10] Generally, a gadolinium-based contrast agent (GBCA) is administered in this technique, and a T2- or T2*-weighted MRI sequence is applied. GBCA causes signal loss due to its paramagnetic effects on T2*-weighted imaging. The signal loss from the contrast circulation in the vessels and enhancing tissues can be tracked after bolus administration of GBCA.[1,7,8] DSC perfusion allows measurement of several quantifiable parameters such as CBF, CBV, MTT, and TTP, and qualitatively allows us to understand the dynamic perfusion changes in part of the brain or in a lesion, which can be used for several clinical indications such as evaluating cerebral ischemia, distinguishing neoplastic processes from nonneoplastic processes, or particularly differentiating pseudoprogression from true tumor progression in brain tumors.[1,2,4-6,8-10]

Received May 25, 2024; accepted after revision August 28.

From the University of Minnesota Medical School (C.E.B.), Minneapolis, Minnesota; Department of Radiology (C.D.), Hacettepe University, Faculty of Medicine, Ankara, Turkiye; Department of Radiology (O.T.), Yeditepe University, Faculty of Medicine, Istanbul, Turkiye; Center for Clinical Imaging Research (M.W.), University of Minnesota, Minneapolis, Minnesota; and Department of Radiology (A.S., M.F., C.Ö.), University of Minnesota Medical School, Minneapolis, Minnesota.

Please address correspondence to Can Özütemiz, 420 Delaware St, SE, MMC 292, Minneapolis, MN 55455; e-mail: ozutemiz@umn.edu; @CanOzutemiz; @UMNRadiology

http://dx.doi.org/10.3174/ajnr.A8513

SUMMARY

PREVIOUS LITERATURE: DSC was performed in 8 healthy volunteers by using a non–FDA-approved 7T MRI system. A DSC perfusion technique in a clinically approved 7T MRI system has been described in a review article. A unique spin-echo DSC perfusion method at 7T in healthy volunteers has been described. A research-only head coil to utilize 7T DSC perfusion in 4 patients has been used. Given the limited evidence on the clinical validity, practicability, and availability of DSC perfusion at 7T, clinicians and radiologists are reluctant to order 7T MRI studies for diagnosis and follow-up of patients with brain tumors.

KEY FINDINGS: Exporting and postprocessing of high-resolution 7T DSC perfusion data took approximately 30 minutes to several hours. Quantitative parameters could be measured, and high-resolution perfusion maps could be generated. For example, normalized ratios of rCBV were mainly consistent in each anatomic area, and the overall CBV map quality was mostly reasonably good or excellent.

KNOWLEDGE ADVANCEMENT: Despite limitations with postprocessing issues such as increased time and software crashes, 2D gradient-echo EPI DSC perfusion at 7T can be reliably performed by using half-dose contrast, allowing measurement of quantitative parameters and generation of excellent or reasonably good fused high-resolution perfusion maps in axial and coronal planes.

Although a 7T MRI system has been FDA approved for clinical brain imaging since 2017, the information regarding the utility and practicality of DSC perfusion at 7T is markedly limited. The most recent American Society of Functional Neuroradiology (ASFNR) recommendation for the clinical performance of DSC perfusion does not discuss the utility of 7T.[1] According to this white paper, 3T has the advantage over 1.5T regarding DSC perfusion because it provides greater CBV map quality and SNR due to increased susceptibility artifacts from the magnetic strength. To our knowledge, only 4 reports utilized DSC perfusion at 7T. Knutsson et al[11] first performed DSC perfusion in 8 healthy volunteers by using a non–FDA-approved 7T MRI system. Second, Özütemiz et al[12] described their DSC perfusion technique in a clinically approved 7T MRI system in a review article. Third, Elschot et al[13] described a unique spin-echo DSC perfusion method at a 7T MRI system in 41 healthy volunteers as part of a research project instead of using a traditional gradient-echo sequence. Finally, Wongsawaeng et al[14] utilized 7T DSC perfusion in 4 patients by using a research-only head coil.

Given the limited evidence on the clinical validity, practicability, and availability of DSC perfusion at 7T, clinicians and radiologists are reluctant to order 7T MRI studies for diagnosis and follow-up of patients with brain tumors. This study aims to determine if DSC perfusion MRI obtained at a clinical 7T MRI system is feasible from a practical and technical point of view in a real patient care setting.

MATERIALS AND METHODS

This retrospective study was approved by the University of Minnesota Medical Center's institutional review board. Between January 2023 and December 2023, 13 patients with DSC perfusion at 7T were identified through institutional PACS.

All 7T MRIs were obtained with an FDA-approved clinical system, 7T Magnetom Terra scanner (Siemens) equipped with 1-channel transmit and 32-channel receive array Nova head coil (Nova Medical). For all cases, a half-dose (0.05 mL/kg) of standard GBCA (Gadavist, Bayer) was administered with hand-injection method via 20 or 22G butterfly-type intravenous access through antecubital fossa. There was no specific arm preference, and no GBCA preloading was applied. In-house–made calcium titanate dielectric bags with a 3:1 ratio, prepared per previously published reports,[15-17] were placed in the bitemporal regions, and a commercially available calcium titanate dielectric bag pad (Multiwave Imaging) was placed in the suboccipital region for each case. Image acquisition started 45 seconds before contrast injection, followed by a saline flush. DSC perfusion sequence parameters at 7T Magnetom Terra are provided in Table 1. For comparison, clinically used DSC perfusion sequence parameters in our institution at 3T Skyra and 1.5T Aera machines (Siemens) are also provided in Table 1.

Each MRI examination, including gray-scale source perfusion data, was exported in DICOM format from PACS to FDA-approved SyngoVIA software (Siemens), which is the standard software we routinely use from any workstation in our institution for DSC perfusion MRI postprocessing. If SyngoVIA software crashed or failed to do the postprocessing, images were then sent to a second FDA-approved software (DynaSuite; MeVis) in a dedicated single workstation to do the postprocessing. Using an automatic motion correction algorithm, standard relative CBV (rCBV), relative CBF (rCBF), relative MTT (rMTT), and relative TTP (rTTP) maps were created in 9 patients. These were fused with contrast-enhanced 3D T1-MPRAGE 7T MR images and sent to PACS in axial and coronal reconstructions for qualitative observer assessment.

In patients with adequate contrast boluses, mean and maximum rCBV, rMTT, rCBF, and rTTP values were quantitively measured from corresponding perfusion maps by using a standard 1 cm^2 round-shaped region-of-interest generated by a radiology resident. An attending board-certified neuroradiologist checked all these maps and measurements. Five anatomic locations were selected for measurement bilaterally, including the middle frontal gyral cortex, precentral gyrus hand motor cortex, thalamus, occipital gyrus, and corona radiata to represent normal-appearing white matter (NAWM) (Fig 1). In patients with intracranial enhancing target lesions, quantitative measurements were obtained from these specific target lesions. A

Table 1: Comparison of dynamic susceptibility contrast-enhanced perfusion sequence parameters in different magnetic field strengths in our institution[a]

	7T	3T	1.5T
Machine	Terra	Skyra	Aera
Head coil	**1tx/32rx Nova**	**20-channel head and neck coil**	**20-channel head and neck coil**
Sequence	2D GRE-EPI	2D GRE-EPI	2D GRE-EPI
Imaging plane	Axial	Axial	Axial
Slice thickness	**1.6 mm**	**5 mm**	**5 mm**
Matrix	**146 × 146**	**128 × 100**	**128 × 100**
Field of view	225 mm	230 mm	230 mm
Interslice distance	**0%**	**40%**	**20%**
Voxel size	**1.5 × 1.5 × 1.6 mm^3**	**1.8 × 1.8 × 5 mm^3**	**1.8 × 1.8 × 5 mm^3**
# of axial slices	**84**	**21**	**27**
TR/TE	**1500/24 ms**	**2300/43 ms**	**2300/30 ms**
Excitation flip angle	80	90	90
Fat-saturation flip angle	110	None	None
Slice acceleration	3	None	None
Imaging time points	**120**	**60**	**60**
Total acquisition time	**3.24 minutes**	**2.24 minutes**	**2 minutes**
Data size	**3.7 GB**	**252 MB**	**250 MB**
Postprocessing time	**45 minutes to 2 hours**	**5–10 minutes**	**5–10 minutes**

[a] Markedly different parameters are highlighted in Bold.

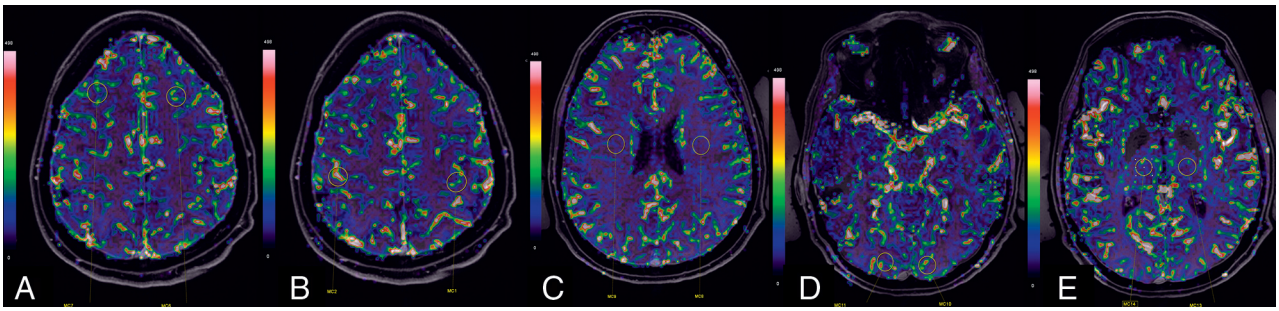

FIG 1. Example of measurements from bilateral anatomic target areas on fused rCBV map. *A*, Middle frontal gyrus cortex. *B*, Precentral gyrus cortex. *C*, Bilateral corona radiata. *D*, Occipital cortex. *E*, Thalamus.

medical student entered all data into a data spreadsheet for further analysis.

Two board-certified neuroradiologists with at least 2 years of experience interpreting clinical 7T MRI scans in a tertiary academic center reviewed each axial and coronal perfusion map in a consensus meeting to assess susceptibility artifacts and overall map quality. Susceptibility artifacts were ranked on a scale of 1 to 5 (1: no susceptibility artifact, 2: mild, 3: moderate, 4: moderate to severe, 5: severe). Map quality was ranked on a scale of 1 to 5 (1: excellent, 2: reasonably good, 3: adequate, 4: suboptimal, 5: poor). Enhancing target lesions were visualized and qualitatively characterized as tumor progression, treatment effect, or indeterminant based on their perfusion MRI findings by the neuroradiologists on consensus. The neuroradiologists were also asked to qualitatively compare the resolution and quality of the fused axial and coronal perfusion maps at 7T MRI relative to their institutional standard 3T and 1.5T MR perfusion maps.

Statistical Methods

The maximum and mean values of rCBV, rCBF, rMTT, and rTTP were normalized by dividing each measurement by its corresponding maximum or mean value measured in the ipsilateral corona radiata. Descriptive statistics were calculated, including mean, median, and interquartile ranges. All statistical analyses and boxplots were generated by using SPSS v.29 (IBM). A descriptive analysis of the Likert scale for susceptibility artifact and imaging quality was performed.

RESULTS

Exporting each scan from PACS to postprocessing software took variable time, approximately 30 minutes to several hours, with each platform crashing often during data upload. Especially if multiple examinations were exported simultaneously, the network and software could not handle the data load. Therefore, each examination was exported to the abovementioned platforms on separate days. Four of the 13 patients initially selected had to be excluded due to poor manual contrast bolus or system failures; thus, the software could not generate the perfusion maps. Five cases were uploaded to SyngoVia, and 4 were uploaded to DynaSuite for analysis. After data export, data postprocessing took roughly 10–15 minutes. A total of 9 patients (age range: 25–82, average age: 52, 5 women) with 7T DSC perfusion MRIs were included for final analysis. Indications for included patients were: included intracranial aneurysm, concern for viral encephalitis, seizure disorder with glioma, adenocarcinoma of the esophagus

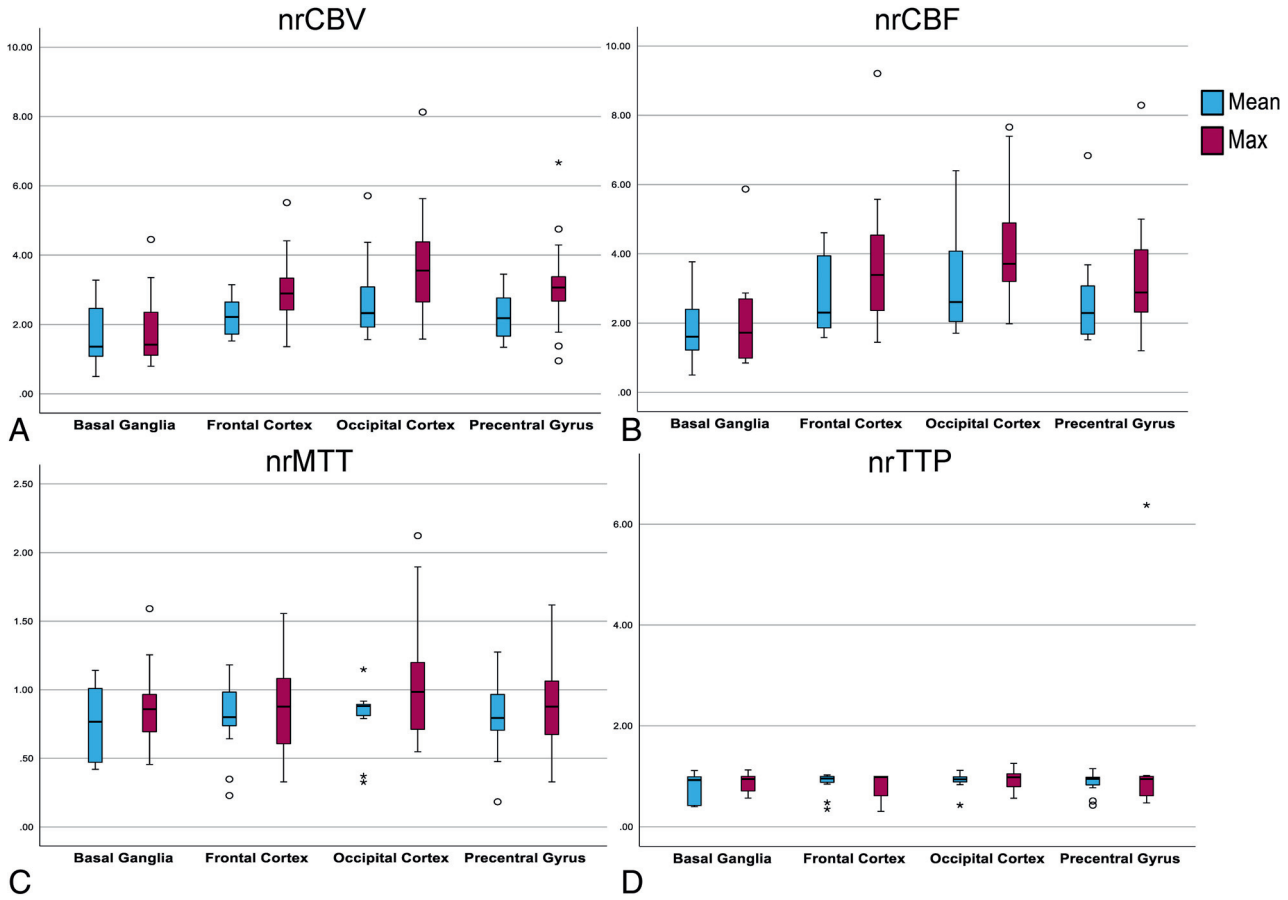

FIG 2. Boxplots for nrCBV (*A*), nrCBF (*B*), nrMTT (*C*), nrTTP (*D*), nrCBV, nrCBF, nrMTT, and nrTTP values are calculated from the means and maximums of rCBV, rCBF, rMTT, and rTTP values measured from each anatomic location relative to ipsilateral NAWM. Middle lines represent median values, boxes represesnt interquartile ranges first and third, and whiskers represent minimum and maximum values. *A*, Overall, nrCBV is largely consistent in each anatomic area with limited dispersion and outliers. *B*, nrCBF for each anatomic location is largely consistent with some increased dispersion and some increased ranges of data, especially in the occipital cortex. *C*, nrMTT is overall consistent; however, there is a large dispersion and ranges of values, especially in the frontal cortex and occipital cortex. *D*, nrTTP is consistent across all anatomic areas with little dispersion.

with new dizziness, refractory benign childhood epilepsy with centrotemporal spikes, metastatic epithelioid trophoblastic neoplasm, metastatic lung cancer, focal partial idiopathic epilepsy, and grade 4 astrocytoma. Two of the 9 patients had enhancing lesions on anatomic imaging. Normalized ratios of rCBV (nrCBV), rCBF (nrCBF), rMTT (nrMTT), and rTTP (nrTTP) were calculated as a ratio of the means and maximums of each anatomic area to NAWM. Boxplots of each of these normalized values were generated and are displayed in Fig 2. For nrCBV, values at each anatomic area were consistent, with some increased variability at the precentral gyrus. There was little dispersion or outliers in the nrCBV data. For nrCBF, values at each anatomic area were also consistent, but data were somewhat more dispersed, as indicated by larger interquartile ranges and increased ranges, especially in the occipital cortex. For nrMTT, values at each anatomic area were consistent, but there was a wide dispersion of data across all anatomic areas. Additionally, the nrMTT data had numerous outliers, especially in the occipital and frontal cortexes. The nrTTP values were the most consistent, with little variability across all the anatomic areas.

Susceptibility artifacts varied from none to moderate/severe for the cerebellum (mostly mild), from mild to moderate/severe for the temporal lobe (mostly moderate), from mild to moderate/severe for the brainstem (mostly mild), from minimal to moderate for the basal ganglia (mostly moderate), and none to mild in the frontal, occipital, and parietal gyri (almost always none) (Table 2).

Overall map quality varied from excellent to adequate for CBV (mostly reasonably good), from excellent to reasonably good for CBF (mostly excellent), excellent to adequate for MTT (mostly reasonably good), and excellent to reasonably good for TTP (mostly reasonably good) (Table 3). Both neuroradiologists agreed that the 7T fused images were better in resolution and quality than their institutional 3T fused DSC perfusion images in axial and coronal planes.

A total of 6 target lesions were measured in 2 different patients. All 6 lesions were well or excellently visualized on fused perfusion maps. Only in a single patient was a follow-up DSC perfusion MRI available at 3T; therefore, a direct comparison of 7T and 3T can be made only in that particular case (Fig 3). Three of the lesions were characterized as tumor progression, 1 lesion was classified as indeterminant, and 2 lesions were classified as radiation necrosis. In the first patient with a history of grade 4 astrocytoma, status postsurgical debulking, radiation therapy,

Table 2: Likert scale ratings of susceptibility artifacts for selected anatomic areas based on consensus agreement

Case	Cerebellum	Temporal Lobe	Brainstem	Basal Ganglia	Frontal Gyri	Occipital and Parietal Gyri
1	2	3	3	4	1	1
2	1	3	2	3	1	1
3	2	3	2	3	1	1
4	1	2	2	3	1	1
5	3	3	2	2	2	1
6	2	2	2	3	2	1
7	2	3	2	4	2	1
8	4	4	4	3	2	1
9	2	3	2	3	2	2
Average score	2.1	2.89	2.3	3.1	1.5	1.1

Note:—Overall artifact score rating: 1 = none, 2 = mild, 3 = moderate, 4 = moderate/severe, 5 = severe.

Table 3: Likert scale ratings for rCBV, rCBF, rMTT, and rTTP overall map quality based on consensus agreement

Case	rCBV	rCBF	rMTT	rTTP
1	2	2	3	2
2	2	1	1	1
3	1	1	1	1
4	1	1	1	1
5	2	1	2	2
6	2	1	2	2
7	2	1	1	1
8	2	2	2	2
9	3	2	2	2
Average score	1.89	1.33	1.67	1.56

Note:—Overall map score rating: 1 = excellent, 2 = reasonably good, 3 = adequate, 4 = sub-optimal, 5 = poor.

and chemotherapy, 7T MRI depicted 3 enhancing target lesions and based on DSC perfusion MRI, lesion 1 was defined as radiation necrosis, lesion 2 as tumor progression, and lesion 3 as indeterminant by the neuroradiologists. Based on multiple follow-up MRI examinations, lesion 2 grew markedly over time, and it was confirmed as true tumor progression with biopsy, while the others got smaller and were confirmed as treatment effect (Fig 3). In the second patient with a history of glioma and radiation therapy, 7T MRI depicted 2 new enhancing lesions in the basal ganglia with markedly increased rCBV (Lesion 1-$rCBV_{max}$:364, Lesion 2-$rCBV_{max}$:492), which were considered as progressive disease, while there was an enhancing focus that remained stable on multiple priors without increased rCBV on DSC (Lesion 3-$rCBV_{Max}$:227), regarded as radiation necrosis (Contralateral NAWM-$rCBV_{Max}$:234). Unfortunately, the patient decided to go to hospice. Therefore, no follow-up imaging with perfusion or autopsy confirmation could be obtained, and the patient died within 3 months.

DISCUSSION

Increasing the magnetic field strength increases the magnetic susceptibility effect and improves the resolution and sensitivity of DSC perfusion.[1-10] Almost all clinical literature regarding the usage of DSC perfusion is based on studies performed at 1.5T and 3T; thus, the clinical utility of DSC perfusion at 7T is unknown. Only 3 reports describe the utility of 2D gradient echo (GRE) GRE-EPI DSC perfusion at 7T with small sample sizes.[11,12,14] A unique spin-echo DSC perfusion technique at 7T has also been recently described in healthy elderly volunteers.[13]

In this study, we used the technique previously described by our group and tried to validate the sequence parameters further in real clinical practice by using a clinically approved system.[12] With the lack of data on DSC perfusion at 7T MRI, the first part of our investigation focused on its feasibility. Measuring, calculating, and comparing nrCBV, nrCBF, nrMTT, and nrTTP values, we determined that these values could be measured reliably at 7T. Thus, DSC perfusion at 7T is possible. Similar to the increased utility of 3T compared with 1.5T, our study illustrated that DSC perfusion at 7T generates qualitatively better perfusion maps at higher resolution. At our institution, 3T and 1.5T DSC perfusion examinations are traditionally obtained by using a 2D GRE-EPI sequence with the parameters detailed in Table 1. While the in-plane resolution is sufficient, the lower resolution along the z-axis at 3T could be a substantial obstacle, particularly when generating fused postcontrast T1-MPRAGE images with rCBV maps in the coronal plane, causing obvious staircase artifacts as seen in Fig 3. This limitation in the resolution and partial volume effect may limit the radiologist in discrimination of the normal cortical perfusion activity from a true lesion perfusion or the differential diagnosis of tumor recurrence from radiation necrosis based on the orientation of the lesion in the axial plane. Our study shows that generating rCBV maps with 1.5 × 1.5 × 1.6 mm^3 voxel size is possible, thus allowing high-resolution anatomic MR images to be fused at different planes with perfusion data by using current clinical 7T MRI systems (Fig 3).

To our knowledge, Knutsson et al[11] utilized DSC perfusion at 7T for the first time in 8 healthy volunteers by using a research-only Achieva 7T MRI machine (Philips) equipped with a 32-channel phased-array head coil (Nova Medical). Participants received a full dose of GBCA approximately 9 minutes before perfusion as part of a separate research project. A half-dose of GBCA was later administered for the DSC perfusion sequence, with the following parameters: 2D GRE-EPI sequence, TR/TE: 1500/30 ms, flip angle: 70°, in-plane resolution: 2 × 2 mm^2, slice thickness: 3 mm, voxel size: 2 × 2 × 3 mm^3, time points: 120, acceleration factor: 2. The authors did not report the total scan time, the software used for postprocessing, or how long it took to do the postprocessing. While the authors could generate perfusion maps comparable to clinical and research scans at 3T, they did not assess any pathology in this small cohort. Our technique's advantages over this study are improved resolution, FDA-approved 7T MRI system usage, and lack of GBCA preloading.

Wongsawaeng et al[14] also utilized DSC perfusion in 4 patients by using a 7T Terra equipped with a research-only 8-channel phased-array transmit/receive RF head coil (Rapid Biomedical) and standard dose GBCA administration. Their DSC perfusion

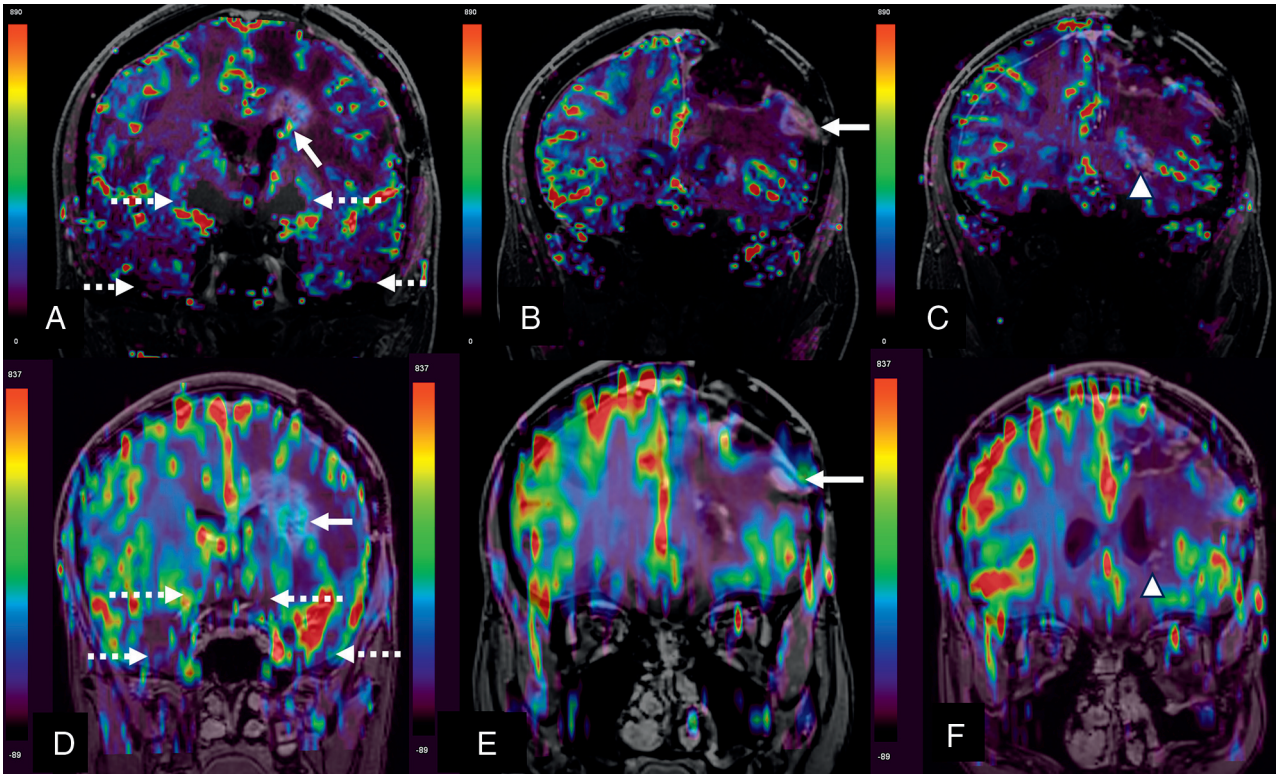

FIG 3. Comparison of 7T DSC perfusion MRI and 3T DSC perfusion in patient 1, a 34-year-old woman with *IDH1*-mutant, *MGMT*-promoter-methylated World Health Organization grade 4 astrocytoma, status postsurgical debulking, radiation therapy, and chemotherapy with temozolomide and lomustine. Coronal reconstructions of 7T fused CBV map with contrast-enhanced 3D T1-MPRAGE are shown (*A–C*). *D–F*, show coronal reconstructions of 3T fused CBV map with contrast-enhanced 3D T1-MPRAGE, obtained 5 months later. *A*, *Solid arrow* depicts an enhancing periventricular lesion posterior and inferior to the surgical cavity with visually increased rCBV in the inferior enhancing component ($rCBV_{max} = 237$), designated as tumor progression visually by the neuroradiologists. *Dashed arrows* represent susceptibility-related low signals near the skull base. *B*, *Solid arrow* shows enhancement in the inferior aspect of the resection margins without visually increased rCBV ($rCBV_{max} = 137$), designated as treatment effect. *C*, *Arrowhead* points to a new enhancing nodular focus in the ventral periventricular white matter, demonstrating similar contrast enhancement to the lesion in (*A*), with questionable visually increased rCBV ($rCBV_{max} = 188$). Although perfusion findings were not highly suspicious, because of new occurrence and nodularity, radiologists defined this lesion as indeterminant. (contralateral corona radiata $rCBV_{max} = 63$, contralateral frontal cortex $rCBV_{max} = 346$) *D*, *Solid arrow* represents progression of lesion seen in (*A*) with increased size and visually increased internal perfusion. This lesion was biopsied and confirmed as tumor progression. *Dashed arrows* represent increased susceptibility-related low signal near the skull base, still present at 3T but less conspicuous compared with 7T. Significant staircase artifacts are present at 3T coronal maps compared with 7T, with false increased perfusion superimposed on calvaria. *E*, *Solid arrow* depicts decreased size of enhancing lesion inferior to the resection cavity without visible increased rCBV, corresponding to the *solid arrow* in (*B*), confirming treatment effect. *F*, *Arrowhead* depicts decreased size of enhancing lesion in (*C*) without any visibly increased rCBV, confirming treatment effect.

sequence parameters are as follows: 2D GRE-EPI sequence, TR/TE: 1500/20 ms, flip angle: 20°–45°, field of view: 192 mm^2, matrix: 64×64, axial slices: 24, slice thickness: 2 mm (0.6 mm gap), voxel size: $3 \times 3 \times 2.6$ mm^3, scan time: 4.20 minutes. All perfusion analysis was performed by using FDA-approved NordicBrainEx software (NordicNeuroLab). The authors did not describe how many time points were acquired or how long it took to postprocess perfusion images. Regardless, they could generate high-quality and high-resolution perfusion maps, and they were able to demonstrate increased rCBV in tumor regions relative to NAWM by using a low flip angle technique. The advantages of our method over this study are improved resolution, decreased scan time, FDA-approved head coil usage, and half-dose contrast usage. Although the authors did not report the number of acquired time points or postprocessing times, given their low matrix and low number of axial slices, the data size would presumably be smaller. Eventually, postprocessing time is also expected to be shorter than ours.

Elschot et al[13] recently described a unique spin-echo DSC perfusion technique at 7T in 41 elderly volunteers by using a 7T MRI system equipped with a 32-channel phased array coil as part of a research study. The perfusion data were postprocessed by using non–FDA-approved software. Interested readers should refer to the cited paper for details of the sequence parameters. However, published perfusion map images had poor resolution (matrix: 96×96), and this technique did not describe any clinical experience. Therefore, this method may not be feasible for routine clinical practice.

While the increased magnetic strength favors improved resolution and image quality, the same phenomenon increases

susceptibility at the skull base, leading to a lack of signal and perfusion information. Our small sample shows this phenomenon is almost negligible in the frontal, parietal, and occipital regions. At the same time, basal ganglia and inferior temporal lobes are most affected, with the degree of artifacts at a moderate level. Therefore, the assessment of lesions in these regions can be limited at DSC. While the same phenomenon can also be an issue at 3T, our study does not do a side-by-side comparison of 3T and 7T regarding DSC, but as seen in Fig 3, these artifacts are more pronounced at 7T compared with 3T.

The most crucial practical limitation of DSC perfusion at 7T is the large data size, longer data transfer, and longer postprocessing times compared with 3T. In many circumstances, the network could not tolerate large data transfers to postprocessing software, leading to software crashes or significantly longer computation times than expected. Thus, our study could not accurately measure the consumed time for each case. These issues are the central problem in the practical application of DSC perfusion at 7T MRI in a busy clinical center. The extensive data size can be lowered by decreasing the matrix, slice thickness, or time points. However, 7T allows unique high-resolution imaging, particularly within the z-direction. Without losing this gain, decreasing the time points, perhaps down to 60 or 80, appears to be a potential solution. Future research should focus on improving the postprocessing time.

Several limitations were present in this study. Overall, our sample size of 9 successful measurements was small. Additionally, our study only examined lesion characterization for 6 lesions in 2 cases. Despite the small size, this is the first and largest validation study performed by using a clinical 7T MRI system in a clinical patient setting. With these promising results from these first cases, we look forward to conducting more DSC perfusion in brain tumor cases. Because we had a small cohort, we did not consider performing a blind review of each study to assess interobserver variability. Therefore, a κ analysis was not performed. Another limitation is the lack of automatic power contrast injector usage. When we started DSC perfusion, we did not have a 7T MRI-compatible power injector available, but when we were writing this paper, our institution purchased a 7T-compatible power injector. We also used a slightly high flip angle for image acquisition. The ASFNR white paper recommends a low flip angle usage for DSC perfusion.[1] Knutsson et al[11] and Wongsawaeng et al[14] also used lower flip angles in their study. We plan to lower our flip angle from 80° to 60° or 70° in the future, correlating with Knutsson et al[11] and ASFNR white paper.[1]

CONCLUSIONS

Despite limitations with postprocessing issues such as increased time and software crashes, measuring nrCBV, nrCBF, nrMTT, and nrTTP values reliably with DSC perfusion at clinical 7T MRI systems is possible. Excellent or reasonably good fused perfusion maps can be generated with high resolution in both axial and coronal planes. While susceptibility artifacts are more pronounced than 3T and can be a limiting factor in the lower temporal regions, brainstem, and basal ganglia, DSC perfusion at 7T can depict tumor progression or radiation necrosis. Our results indicate that DSC perfusion at 7T MRI is a clinically available and useful tool, providing better resolution than at 1T and 3T. Improvements in data acquisition, postprocessing software, and network systems may increase the clinical utility of 7T DSC perfusion.

Disclosure forms provided by the authors are available with the full text and PDF of this article at www.ajnr.org.

REFERENCES

1. Welker K, Boxerman J, Kalnin A, et al; American Society of Functional Neuroradiology MR Perfusion Standards and Practice Subcommittee of the ASFNR Clinical Practice Committee. **ASFNR recommendations for clinical performance of MR dynamic susceptibility contrast perfusion imaging of the brain.** *AJNR Am J Neuroradiol* 2015;36:E41–51 CrossRef Medline
2. Barajas RF, Chang JS, Sneed PK, et al. **Distinguishing recurrent intra-axial metastatic tumor from radiation necrosis following gamma knife radiosurgery using dynamic susceptibility-weighted contrast-enhanced perfusion MR imaging.** *AJNR Am J Neuroradiol* 2009;30:367–72 CrossRef Medline
3. Hiremath SB, Muraleedharan A, Kumar S, et al. **Combining diffusion tensor metrics and DSC perfusion imaging: can it improve the diagnostic accuracy in differentiating tumefactive demyelination from high-grade glioma?** *AJNR Am J Neuroradiol* 2017;38:685–90 CrossRef Medline
4. Wintermark M, Sanelli PC, Albers GW, et al. **Imaging recommendations for acute stroke and transient ischemic attack patients: a joint statement by the American Society of Neuroradiology, the American College of Radiology, and the Society of NeuroInterventional Surgery.** *AJNR Am J Neuroradiol* 2013;34:E117–27 CrossRef Medline
5. Apruzzese A, Silvestrini M, Floris R, et al. **Cerebral hemodynamics in asymptomatic patients with internal carotid artery occlusion: a dynamic susceptibility contrast MR and transcranial Doppler study.** *AJNR Am J Neuroradiol* 2001;22:1062–67 Medline
6. Barajas RF, Jr, Chang JS, Segal MR, et al. **Differentiation of recurrent glioblastoma multiforme from radiation necrosis after external beam radiation therapy with dynamic susceptibility-weighted contrast-enhanced perfusion MR imaging.** *Radiology* 2009;253:486–96 CrossRef Medline
7. Essig M, Nguyen TB, Shiroishi MS, et al. **Perfusion MRI: the five most frequently asked clinical questions.** *AJR Am J Roentgenol* 2013;201:W495–510 CrossRef Medline
8. Petrella JR, Provenzale JM. **MR perfusion imaging of the brain: techniques and applications.** *AJR Am J Roentgenol* 2000;175:207–19 CrossRef Medline
9. Copen WA, Schaefer PW, Wu O. **MR perfusion imaging in acute ischemic stroke.** *Neuroimaging Clin N Am* 2011;21:259–83 CrossRef Medline
10. Gordaliza PM, Mateos-Perez JM, Montesinos P, et al. **Development and validation of an open source quantification tool for DSC-MRI studies.** *Comput Biol Med* 2015;58:56–62 CrossRef Medline
11. Knutsson L, Xu X, Stahlberg F, et al. **Dynamic susceptibility contrast MRI at 7 T: tail-scaling analysis and inferences about field strength dependence.** *Tomography* 2017;3:74–78 CrossRef Medline
12. Ozutemiz C, White M, Elvendahl W, et al. **Use of a commercial 7-T MRI scanner for clinical brain imaging: indications, protocols, challenges, and solutions-a single-center experience.** *AJR Am J Roentgenol* 2023;221:788–804 CrossRef Medline
13. Elschot EP, Backes WH, van den Kerkhof M, et al. **Cerebral microvascular perfusion assessed in elderly adults by spin-echo dynamic susceptibility contrast MRI at 7 Tesla.** *Tomography* 2024;10:181–92 CrossRef Medline

14. Wongsawaeng D, Schwartz D, Li X, et al. **Comparison of dynamic susceptibility contrast (DSC) using gadolinium and iron-based contrast agents in high-grade glioma at high-field MRI.** *Neuroradiol J* 2024;37:473–82 CrossRef Medline
15. Fagan AJ, Bitz AK, Bjorkman-Burtscher IM, et al; ISMRM Safety Committee. **7T MR safety.** *J Magn Reson Imaging* 2021;53:333–46 CrossRef Medline
16. Teeuwisse WM, Brink WM, Haines KN, et al. **Simulations of high permittivity materials for 7 T neuroimaging and evaluation of a new barium titanate-based dielectric.** *Magn Reson Med* 2012;67:912–18 CrossRef Medline
17. Teeuwisse WM, Brink WM, Webb AG. **Quantitative assessment of the effects of high-permittivity pads in 7 Tesla MRI of the brain.** *Magn Reson Med* 2012;67:1285–93 CrossRef Medline